Serb. Astron. J. № 194 (2017), 87 - 99
DOI: https://doi.org/10.2298/SAJ160424002C

UDC 523.31-337 : 523.985.3
Professional paper

SOLAR FLARES AND VARIATION OF LOCAL GEOMAGNETIC FIELD: MEASUREMENTS BY THE HUANCAYO OBSERVATORY OVER 2001-2010

Rafael E. Carlos Reyes[1,2], Gabriel A. Gárate Ayesta[1] and Felipe A. Reyes Navarro[2]

[1] *Universidad Nacional del Callao, UNAC, Callao, Peru*

[2] *Universidad Nacional Mayor de San Marcos, UNMSM, Lima, Peru*

E–mail: *felipe.reyes@unmsm.edu.pe*

(Received: April 24, 2016; Accepted: December 13, 2016)

SUMMARY: We study the local variation of the geomagnetic field measured by the Huancayo Geomagnetic Observatory, Peru, during 2001-2010. Initially, we sought to relate the SFI values, stored daily in the NOAA's National Geophysical Data Center, with the corresponding geomagnetic index; however, no relation was observed. Nonetheless, subsequently, a comparison between the monthly geomagnetic-activity index and the monthly SFI average allowed observing a temporal correlation between these average indices. This correlation shows that the effect of the solar flares does not simultaneously appear on the corresponding magnetic indices. To investigate this, we selected the most intense X-class flares; then, we checked the magnetic field disturbances observed in the Huancayo Geomagnetic Observatory magnetograms. We found some disturbances of the local geomagnetic field in the second and third day after the corresponding solar flare; however, the disturbance strength of the local geomagnetic field is not correlated with the X-class of the solar flare. Finally, there are some disturbances of the local geomagnetic field that are simultaneous with the X-class solar flares and they show a correlation with the total flux of the solar flare.

Key words. Earth – Magnetic fields – Sun: flares – Sun: X-rays, gamma rays – Sun: coronal mass ejections (CMEs).

1. INTRODUCTION

From the Carrington flare of September 1859 (Shea et al. 2006), the scientific community boosted research on a relation between the solar activity and disturbances of the geomagnetic field. Nowadays, many investigators consider that there is no direct connection between solar flares and geomagnetic disturbances.

The study of the solar activity in its different manifestations has a very important role because the Sun strongly influences climate, telecommunications and life on Earth (Bai and Sturrock 1989, Cui et al. 2006, Meza et al. 2009). Specially, solar flares are capable of radiating far ultraviolet rays as well as hard and soft x-rays; usually, these flares also are capable of releasing solar material toward the Earth, what eventually produces geomagnetic disturbances (Foukal 2004, Remanan and Unnikrishnan 2014). Furthermore, the geomagnetic activity also stems from several phenomena linked to the interplanetary magnetic field and galactic cosmic rays (Stamper et al. 1999); to the solar wind and coronal

mass ejections (CMEs) (Legrand and Simon 1989a,b, Gosling 1993, Youssef 2012), and to others (Legrand and Simon 1989a,b, Tsurutani et al. 1985, Stamper et al. 1999).

On the other hand, Cliver and Hudson (2002) conclude that it is not well established how the solar flares affect the geomagnetic activities. However, studies carried out by Du and Wang (2012) describe connections between the geomagnetic activity and the parameters of flare; they considered 13 months to be the scale of the mean response time; the delay time between the peaks of both is predicted about 47%. A similar result was found by Howard and Tappin (2005), who, by using CMEs data, found a dependence between the X-class flares and Ap and Dst indices for geomagnetic storms (Dst stands for disturbance storm time). Nonetheless, in these works, a direct connection of the solar flare intensity with the variation of the geomagnetic field was not shown.

To study the geomagnetic field we use the Indices of Global Geomagnetic Activity Ap (Rangarajan 1989, Siebert and Meyer 1996), and to analyze the local geomagnetic field we use magnetograms measured by the Huancayo Geomagnetic Observatory (HGO), which is operated by the Geophysical Institute of Peru, Rosales Corilloclla et al. (2011). The HGO is located at $12°02'28.69''$ south latitude and $75°19'14.11''$ west longitude, with an altitude of 3314 meters above the mean sea level; the HGO has an inclination-declination MAG-01H Fluxgate magnetometer, Bartington model, and a proton precession magnetometer, too. Since the first magnetogram, obtained in March 1922, it was a surprise to find that the diurnal variation of the geomagnetic field was more than twice the expected, and much larger than the observed in other observatories located in similar geographical latitudes (Giesecke and Casaverde 1998).

2. DATA

We have divided the information about the used data into five parts.

2.1. The local geomagnetic field

The values obtained through the HGO magnetograms are recorded every minute, and they are available on the website of the Geophysical Institute of Peru. These data are also sent to the world net of observatories INTERMAGNET, and they are available on its website `http://www.intermagnet.org/data-donnee/dataplot-eng.php`. After a treatise with NOAA, NOAA's NCEI can obtain these data directly from INTERMAGNET and store them in WDC-A; NCEI means National Centers for Environmental Information (NCEI 2015) and WDC-A, World Data Center-A. The former NGDC was recently merged into the NCEI; NGDC stands for National Geophysical Data Center.

The HGO measures the horizontal and vertical components of the geomagnetic field. For this work we have selected magnetograms corresponding to 2001-2010. The monthly selection of the magnetically quietest days and the magnetically most disturbed days (Q-days and D-days, respectively), is based on a statistical criterion of the global geomagnetic storm indices Kp (Mayaud 1980). To find out a possible correlation between solar flares and the geomagnetic field behavior, graphs corresponding to 3 652 days have been studied.

2.2. Undisturbed diurnal variation

To identify the magnetic disturbances corresponding to solar flares, we firstly need to recognize the shape and maximum mean value of the diurnal variation of H in normal quiet days. For this reason, we take as reference values the quiet days stored by the Data Analysis Center for Geomagnetism and Space Magnetism, Kyoto University (DACGSM 2015). For each month this database has ten magnetically quietest days and five magnetically most disturbed days, which allow us to notice the behavior of the diurnal variation in the HGO data and to select those having the least possible disturbance caused by some external phenomenon.

In Fig. 1, we have the shape of the diurnal variation in the magnetic field observed by the HGO. The variation of H, the blue color line, is shown as a steeper curve at local noon, and with a mean amplitude ranging between 100 and 200 nT. By having the mean shape of the diurnal variation in the HGO, we can identify the local geomagnetic-disturbance days during 2001-2010 in the registered magnetograms.

2.3. Flare indices

In searching to quantify the daily flare activity over 24 hours per day, Kleczek (1952) introduced the solar flare index defined as $Q{=}it$, where i represents the intensity scale of importance of a flare in Hα images (Table 1) and t is the flare duration measured in minutes (Knŏska and Petrásek 1984, Ataç and Özgüç 1998). This relationship is assumed to give roughly the total energy emitted by a flare.

Solar flare indices were extracted from the database of the NOAA's NCEI (NOAA-flares 2015), which provided us the flare indices throughout the solar disk during 2001-2010. The annual tables of the flare indices furnished us with the corresponding daily values, the monthly mean, and also the yearly mean over the period being studied. Because the local geomagnetic-field disturbances can be caused by different phenomena, whether atmospheric or solar, we will take into account only the highest data of the flare indices. However, we need to set a minimum value which can be used as a gauge to consider a flare as outstanding. This value is selected by considering the respective highest values of the indicators for the size and brightness representing the flare (Table 1); size and brightness are obtained from the Hα image.

Table 1. Classification of flares by their area and brightness observed in Hα images.

Size of the flare			Bright of the flare
Indicator	Actual area	Apparent area*	Indicators
S	Area<2.0	Area<200	f,n,b
1	2.1<Area<5.1	200<Area<500	f,n,b
2	5.1<Area<12.4	500<Area<1200	f,n,b
3	12.4<Area<24.7	1200<Area<2400	f,n,b
4	Area>24.7	Area>2400	f,n,b

*The actual area is measured in square degrees. The apparent area is measured in millionths of the solar disk.

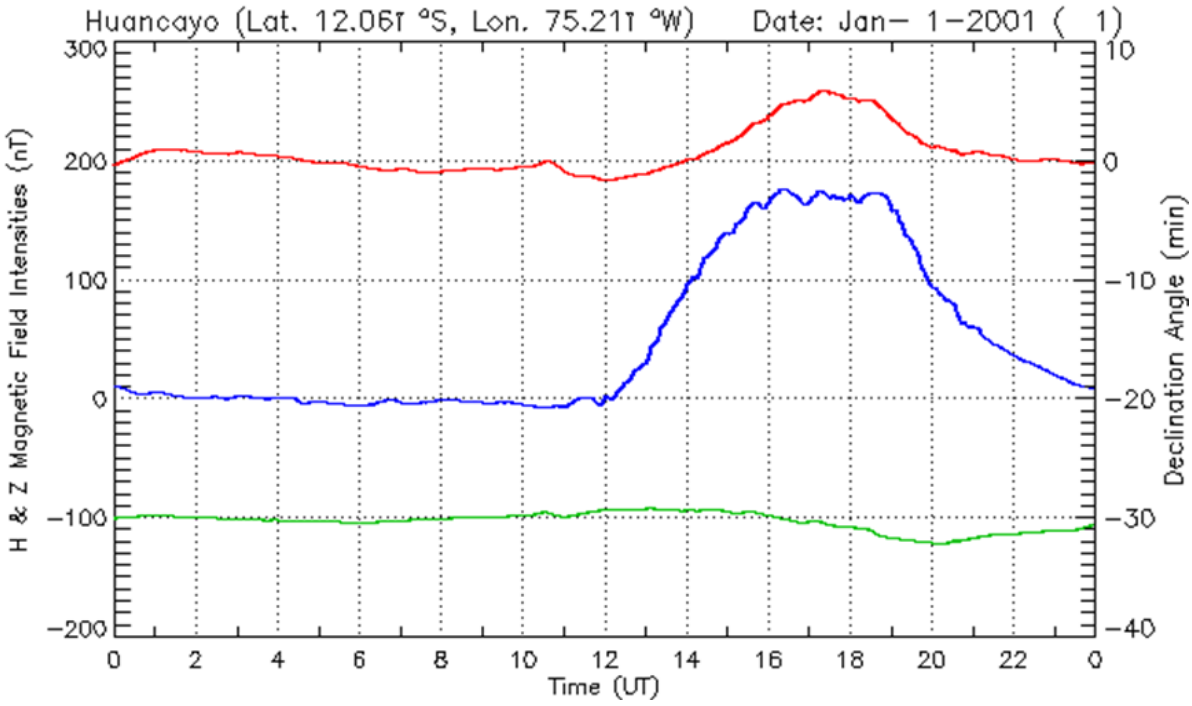

Fig. 1. *Q1-day magnetogram of January 2001 (the first quietest day). The red line corresponds to the declination angle measured in minutes; the blue line, to the horizontal component measured in nanoteslas; the green line, to the vertical component measured in nanoteslas too. This figure was taken from Huancayo Geomagnetic Observatory.*

Table 2. Conversion between the intensity scale of importance and the intensity scale of importance of a flare.

Intensity Scale of Importance of the Flare	Intensity Scale of Importance i
SF, SN, SB	0.5
1F, 1N	1.0
1B	1.5
2F, 2N	2.0
2B	2.5
3F, 3N, 4F	3.0
3B, 4N	3.5
4B	4.0

Table 2 shows the conversion between the intensity scale of importance and the intensity scale of importance of a flare. By considering a flare having the greatest size (4) and one having the greatest brightness (b), we have a flare 4b with optical importance coefficient i=4.0. For a minimum duration of t=1 minute, we get index SFI=4; this reference value limits the study to the brightest flares having area greater than 2400 millionths of the solar disk after elapsing one minute.

2.4. Magnetic activity indices Ap

To study the Earth's magnetic field, we use Kp and Ap indices. The Kp magnetic index is a code associated with the maximum fluctuations of

the geomagnetic-field horizontal component (H) observed in a magnetometer relative to a quiet day; whereas, the Ap magnetic index is a planetary index, which arose from the need to obtain daily information on the global geomagnetic behavior.

To relate the daily performance of the flare index with daily changes of the global magnetic field during 2001-2010, we use as reference the global geomagnetic activity index Ap, daily and monthly (Mayaud 1980), which was obtained from the World Data Center for Geomagnetism, Kyoto University. For the period being studied, we selected 74 dates presenting an index Ap>48, whose value is related to the existence of geomagnetic storms (Remanan and Unnikrishnan 2014). For the HGO magnetograms satisfying this condition, in dates corresponding to a global geomagnetic storm, we verified an anomalous local change in the geomagnetic field registered by the HGO. This selection allows us to relate Ap values with those corresponding to SFI on the same dates (Fig. 2).

2.5. X-class flares

NOAA has a database of solar flares along with its X-ray intensity as a function of time, indicating start, end, and the maximum peak of the flare (NOAA-NGDC 2015). This classification of X-ray flares are X, M, C, B and A according with their strength. In this work, we considered only X-class flares having a large intensive radiation, and presumably a large emission of particles too. In the data collected, we identify 87 X-class flares during 73 dates in the period studied.

3. ANALYSIS AND RESULTS

Seeking clarity, we have separated this section into four blocks.

3.1. Connection between the daily SFI index and HGO magnetograms

For 2001-2010, we found 489 dates wherein SFI>4 holds. For these days we revised the HGO magnetograms, and we detected only 267 days when the local geomagnetic field was disturbed; this represents 54.6% of the data, whereas nearly half (45.4%) did not record a disturbance.

This result indicates that either the value adopted SFI>4 is still too small to ensure that there is a disturbance of the local geomagnetic field or all the flares do not produce disturbances that are detected at the HGO. This detection can also depend on the flare location on the solar disk. Another possible explanation would be that the effect of the flares does not manifest instantly in the HGO magnetometers.

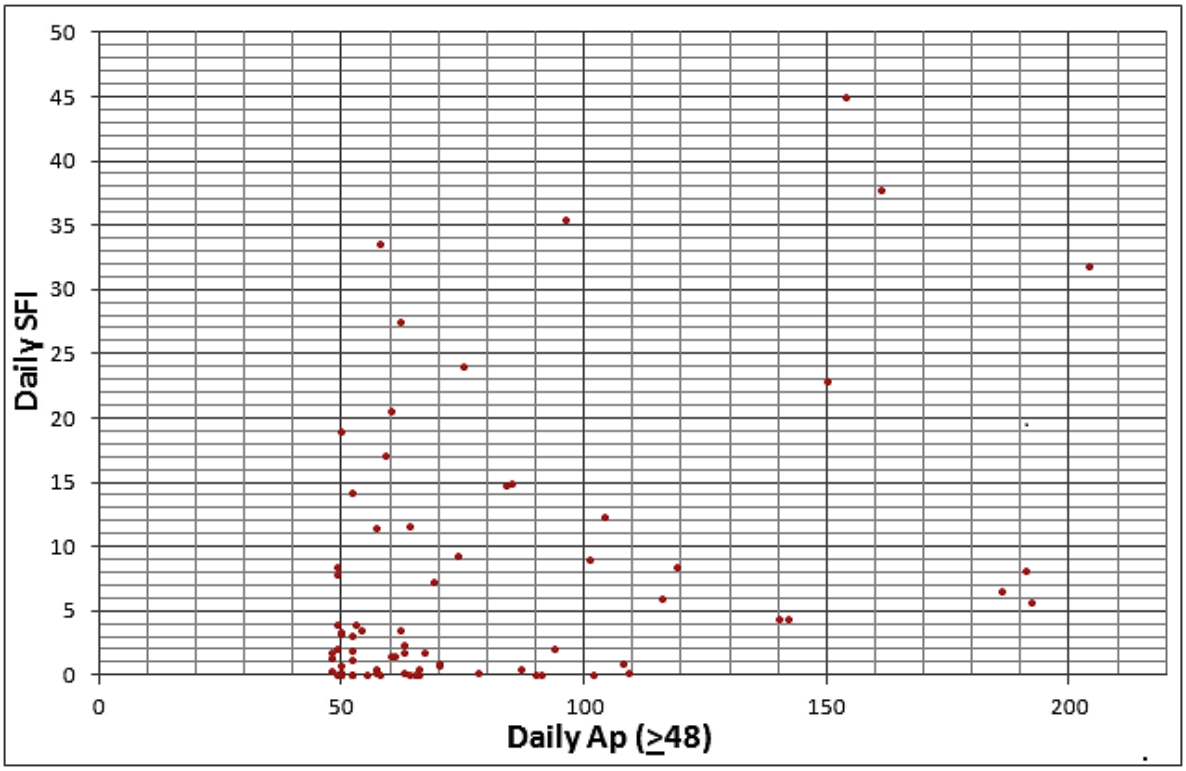

Fig. 2. *Daily Ap values (≥48) corresponding to 74 dates of geomagnetic storms as well as their corresponding SFI indices.*

Therefore, since the flare index does not provide accurate information about the emergence of a flare (such as start and end), this index is not enough to study the local perturbation of the geomagnetic field.

3.2. Connection between daily SFI and Ap indices

For the period being studied, 74 dates having Ap≥48 were selected from the Ap index database. This value is associated with the existence of geomagnetic storms. In analyzing all the days of global geomagnetic storms, we verified that there is an anomalous local behavior in the magnetograms. This allowed us to relate the daily Ap indices with their corresponding SFI indices (Fig. 2). In this figure, we observe that there is no relation between the two data.

Therefore, the daily SFI and Ap indices are not adequate to find any relationship between the two data.

3.3. Connection between monthly SFI and Ap indices

To prove that the events already mentioned are not necessarily simultaneous, we proceed to compare the SFI and Ap indices, but now by using their monthly average. We take the monthly average of both indices and plot them as a function of time; thus, in Fig. 3 we see a strong correlation between the monthly indices, specifically for values of SFI>2 and Ap>10. Although the values of both indices have been reduced because of the monthly mean, we realize that most of the peaks of both indices coincide. Therefore, this result shows that the solar flare events and the local magnetic disturbance are not simultaneous; however, they have a time delay.

One possible explanation is that the discharges triggered by a solar flare, like the release of particles or CMEs, take days to reach the Earth. This would partially explain why 45.4% of the HGO magnetograms shows no disturbance on the same date, even though the daily SFIs have high values.

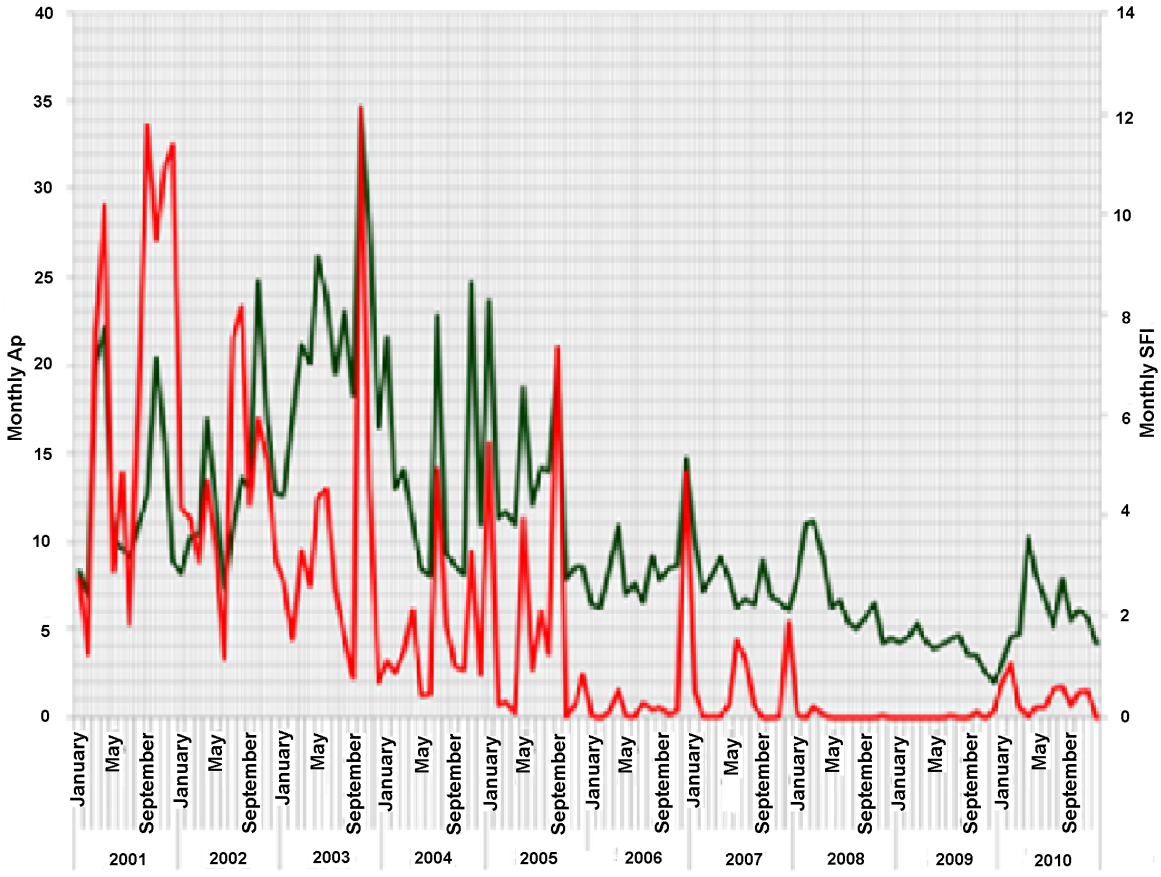

Fig. 3. *Monthly Ap mean (green line) and monthly SFI mean (red line) during 2001-2010.*

Table 3. Dates of X-class flares with their start hour, end hour, and the maximum peak of the flare at UT.

Date (M-D-Y)	Start hour	End hour	Maximum value hour	Class	Date (M-D-Y)	Start hour	End hour	Maximum value hour	Class
03-29-01	09:57	10:32	10:15	X1.7	10-23-03	19:50	20:14	20:04	X1.1
04-02-01	10:04	10:20	10:14	X1.4	10-26-03	05:57	07:33	06:54	X1.2
04-02-01	10:58	12:05	11:36	X1.1	10-26-03	17:21	19:21	18:19	X1.2
04-02-01	21:32	22:03	21:51	X20.0	10-28-03	09:51	11:24	11:10	X17.2
04-03-01	03:25	04:55	03:57	X1.2	10-29-03	20:37	21:01	20:49	X10.0
04-06-01	19:10	19:31	19:21	X5.6	11-02-03	17:03	17:39	17:25	X8.3
04-10-01	05:06	05:42	05:26	X2.3	11-03-03	01:09	01:45	01:30	X2.7
04-12-01	09:39	10:49	10:28	X2.0	11-03-03	09:43	10:19	09:55	X3.9
04-15-01	13:19	13:55	13:50	X14.4	11-04-03	19:29	20:06	19:50	X28.0
06-23-01	04:02	04:11	04:08	X1.2	02-26-04	01:50	02:10	02:03	X1.1
08-25-01	16:23	17:04	16:45	X5.3	07-15-04	01:30	01:48	01:41	X1.8
09-24-01	09:32	11:09	10:38	X2.6	07-15-04	18:15	18:28	18:24	X1.6
10-19-01	00:47	01:13	01:05	X1.6	07-16-04	01:43	02:12	02:06	X1.3
10-19-01	16:13	16:43	16:30	X1.6	07-16-04	10:32	10:46	10:41	X1.1
10-22-01	17:44	18:14	17:59	X1.2	07-16-04	13:49	14:01	13:55	X3.6
10-25-01	14:42	15:28	15:02	X1.3	07-17-04	07:51	07:59	07:57	X1.0
11-04-01	16:03	16:57	16:20	X1.0	08-13-04	18:07	18:15	18:12	X1.0
11-25-01	09:45	09:54	09:51	X1.1	08-18-04	17:29	17:54	17:40	X1.8
12-11-01	07:58	08:14	08:08	X2.8	10-30-04	11:38	11:50	11:46	X1.2
12-13-01	14:20	14:35	14:30	X6.2	11-07-04	15:42	16:15	16:06	X2.0
12-28-01	20:02	21:32	20:45	X3.4	11-10-04	01:59	02:20	02:13	X2.5
04-21-02	00:43	02:38	01:51	X1.5	01-01-05	00:01	00:39	00:31	X1.7
05-20-02	15:21	15:31	15:27	X2.1	01-15-05	00:22	01:02	00:43	X1.2
07-03-02	02:08	02:16	02:13	X1.5	01-15-05	22:25	23:31	23:02	X2.6
07-15-02	19:59	20:14	20:08	X3.0	01-17-05	06:59	10:07	09:52	X3.8
07-18-02	07:24	07:49	07:44	X1.8	01-19-05	08:03	08:40	08:22	X1.3
07-20-02	21:04	21:54	21:30	X3.3	01-20-05	06:36	07:26	07:01	X7.1
07-23-02	00:18	00:47	00:35	X4.8	07-14-05	10:16	11:29	10:55	X1.2
08-03-02	18:59	19:11	19:07	X1.0	07-30-05	06:17	07:01	06:35	X1.3
08-21-02	05:28	05:36	05:34	X1.0	09-07-05	17:17	18:03	17:40	X17.0
08-24-02	00:49	01:31	01:12	X3.1	09-08-05	20:52	21:17	21:06	X5.4
08-30-02	12:47	13:35	13:29	X1.5	09-09-05	02:43	03:07	03:00	X1.1
10-31-02	16:47	16:55	16:52	X1.2	09-09-05	09:42	10:08	09:59	X3.6
03-17-03	18:50	19:16	19:05	X1.5	09-09-05	19:13	20:36	20:04	X6.2
03-18-03	11:51	12:20	12:08	X1.5	09-10-05	16:34	16:51	16:43	X1.1
05-27-03	22:56	23:13	23:07	X1.3	09-10-05	21:30	22:43	22:11	X2.1
05-28-03	00:17	00:39	00:27	X3.6	09-13-05	19:19	20:57	19:27	X1.5
05-29-03	00:51	01:12	01:05	X1.2	09-13-05	23:15	23:30	23:22	X1.7
06-09-03	21:31	21:43	21:39	X1.7	09-15-05	08:30	08:46	08:38	X1.1
06-10-03	23:19	00:12	00:02	X1.3	12-05-06	10:18	10:45	10:35	X9.0
06-11-03	20:01	20:27	20:14	X1.6	12-06-06	18:29	19:00	18:47	X6.5
06-15-03	23:25	00:25	23:56	X1.3	12-13-06	02:14	02:57	02:40	X3.4
10-19-03	16:29	17:04	16:50	X1.1	12-14-06	21:07	22:26	22:15	X1.5
10-23-03	08:19	08:49	08:35	X5.4					

3.4. X-class flares and the variation of the *H* horizontal component of the geomagnetic field

We have found that solar flare events are not necessarily simultaneous with the local perturbation of the geomagnetic field. Thus, we now look at Huancayo data which have disturbances after the date of the corresponding solar flare.

We selected the most intense flares according to their X-class classification; we identified 87 solar flares having a total flux higher than 10^{-4} W/m^2, all in 73 dates during 2001-2010. These solar flares are shown in Table 3. Therein it is indicated the date; start time, end time and maximum peak time (at UT); and the corresponding X-class.

We analyze the HGO magnetograms until three days after each flare. In 52 dates, after the occurrence of a solar flare, we found notable disturbances in the local geomagnetic field (Table 4); likewise, in other 9 dates, three days after the flare (Table 5). This represents approximately 83% of the 73 dates.

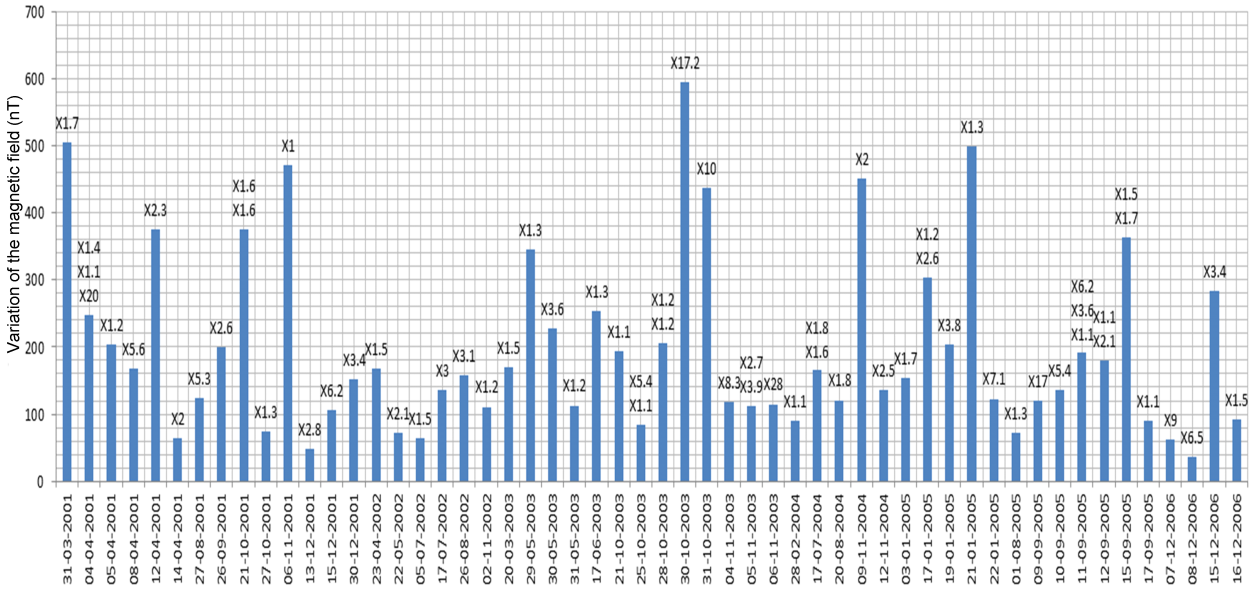

Fig. 4. *Horizontal component's variation, two days after the flares from Table 4. The dates have Day-Month-Year format.*

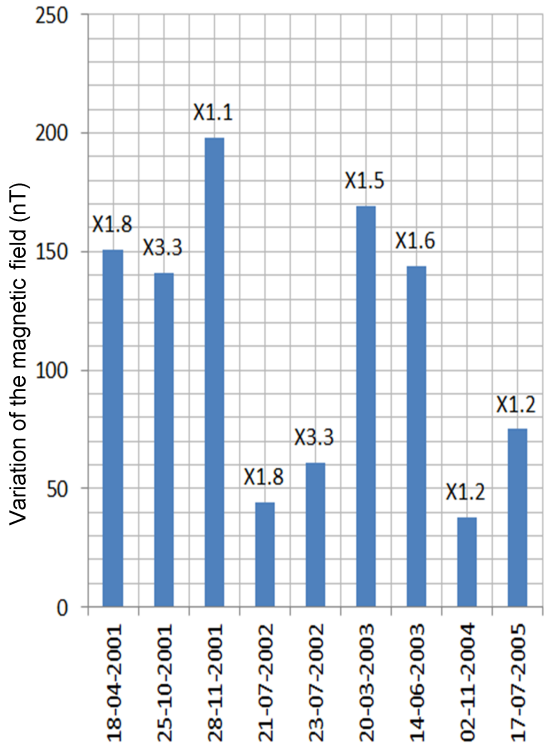

Fig. 5. *Variation of H, horizontal component, three days after the flares from Table 5. The dates have Day-Month-Year format.*

To estimate the maximum disturbance of the geomagnetic field during those days, we compared the different magnetograms with the monthly mean diurnal variation. These changes in the geomagnetic field are shown in Tables 6 and 7, respectively, for two and three days after the corresponding event. From these measurements we realize that these disturbances vary from 36 to 595 nT, corresponding to solar flares classified as X6.5-class and X17.2-class, respectively. The maximum value of the disturbance for each day is shown in the Figs. 4 and 5, corresponding to two and three days after the solar flare, respectively.

Additionally, in observing the HGO magnetograms corresponding to dates of the flares selected from Table 3, in 23 out of 87 cases we observed the emergence of peaks of the variation of H in the time corresponding to the solar flare. For instance, in the upper panel of Fig. 6, we have the peak of the solar flare at 17:40 UT for the X17-class flare on September 7, 2005; whereas in the lower panel of Fig. 6, we find a peak of the disturbance of the geomagnetic field at 17:54 UT in the HGO magnetogram. To view better the result, in Fig. 7 we displayed the start and end of the flare, as well as the time of the peak of the geomagnetic disturbance; it is observed that all peaks are within the flare duration time, whereas in the HGO magnetograms all these events occur within an interval from 09:00 to 24:00 UT. To see if the peak overlapping has a preferential relationship with the flare occurrence location on the solar disk, we proceed to place them on it (Fig. 8). We observe that these flares are mainly located in the southern hemisphere, but they are also located in the northern hemisphere between -30° to 10° longitude, and from -20° to 20° latitude. In Fig. 8, it is also indicated the class of the X-flare and the maximum disturbance of H. No connection of these data with their location on the solar disk is observed.

Table 4. Data wherein a disturbance appeared in the HGO magnetograms 2 days after an X-class flare.

Date (M-D-Y)	Class	Date (M-D-Y)	Class
03-29-01	X1.7	10-28-03	X17.2
04-02-01	X1.4	10-29-03	X10.0
04-02-01	X1.1	11-02-03	X8.3
04-02-01	X20.0	11-03-03	X2.7
04-03-01	X1.2	11-03-03	X3.9
04-06-01	X5.6	11-04-03	X28.0
04-10-01	X2.3	02-26-04	X1.1
04-12-01	X2.0	07-15-04	X1.8
08-25-01	X5.3	07-15-04	X1.6
09-24-01	X2.6	08-18-04	X1.8
10-19-01	X1.6	11-07-04	X2.0
10-19-01	X1.6	11-10-04	X2.5
10-25-01	X1.3	01-01-05	X1.7
11-04-01	X1.0	01-15-05	X1.2
12-11-01	X2.8	01-15-05	X2.6
12-13-01	X6.2	01-17-05	X3.8
12-28-01	X3.4	01-19-05	X1.3
04-21-02	X1.5	01-20-05	X7.1
05-20-02	X2.1	07-30-05	X1.3
07-03-02	X1.5	09-07-05	X17.0
07-15-02	X3.0	09-08-05	X5.4
08-24-02	X3.1	09-09-05	X1.1
10-31-02	X1.2	09-09-05	X3.6
03-18-03	X1.5	09-09-05	X6.2
05-27-03	X1.3	09-10-05	X1.1
05-28-03	X3.6	09-10-05	X2.1
05-29-03	X1.2	09-13-05	X1.5
06-15-03	X1.3	09-13-05	X1.7
10-19-03	X1.1	09-15-05	X1.1
10-23-03	X5.4	12-05-06	X9.0
10-23-03	X1.1	12-06-06	X6.5
10-26-03	X1.2	12-13-06	X3.4
10-26-03	X1.2	12-14-06	X1.5

Table 5. Dates wherein a disturbance in the HGO magnetograms appeared 3 days after an X-class flare.

Date (M-D-Y)	Class
04-15-01	X14.4
10-22-01	X1.2
11-25-01	X1.1
07-18-02	X1.8
07-20-02	X3.3
03-17-03	X1.5
06-11-03	X1.6
10-30-04	X1.2
07-14-05	X1.2

Table 6. The geomagnetic field's maximum variation two days after the dates from Table 4.

Date (M-D-Y)	Class of flare	ΔH (nT)	Date (M-D-Y)	Class of flare	ΔH (nT)
03-31-01	X1.7	-505	10-28-03	X1.2	-206
04-04-01	X20	248	10-30-03	X17.2	-595
04-05-01	X1.2	203	10-31-03	X10	-438
04-08-01	X5.6	-168	11-04-03	X8.3	-118
04-12-01	X2.3	-375	11-05-03	X3.9	-112
04-14-01	X2	64	11-06-03	X28	-115
08-27-01	X5.3	124	02-28-04	X1.1	-91
09-26-01	X2.6	-199	07-17-04	X1.8	-165
10-21-01	X1.6	376	08-20-04	X1.8	-121
10-27-01	X1.3	74	11-09-04	X2	-451
11-06-01	X1	-472	11-12-04	X2.5	-135
12-13-01	X2.8	-49	01-03-05	X1.7	-154
12-15-01	X6.2	106	01-17-05	X2.6	-304
12-30-01	X3.4	-152	01-19-05	X3.8	-204
04-23-02	X1.5	-168	01-21-05	X1.3	499
05-22-02	X2.1	-72	01-22-05	X7.1	-123
07-05-02	X1.5	-64	08-01-05	X1.3	73
07-17-02	X3	136	09-09-05	X17	120
08-26-02	X3.1	158	09-10-05	X5.4	-136
11-02-02	X1.2	-111	09-11-05	X6.2	-191
03-20-03	X1.5	-169	09-12-05	X2.1	-180
05-29-03	X1.3	-346	09-15-05	X1.7	-363
05-30-03	X3.6	-227	09-17-05	X1.1	-90
05-31-03	X1.2	-113	12-07-06	X9	-63
06-17-03	X1.3	-253	12-08-06	X6.5	-36
10-21-03	X1.1	-194	12-15-06	X3.4	-284
10-25-03	X5.4	-84	12-16-06	X1.5	-92

Table 7. The geomagnetic field's maximum variation three days after the dates from Table 5.

Date M-D-Y	Class of flare	ΔH (nT)
04-18-01	X1.8	-151
10-25-01	X3.3	141
11-28-01	X1.1	198
07-21-02	X1.8	44
07-23-02	X3.3	61
03-20-03	X1.5	169
06-14-03	X1.6	144
11-02-04	X1.2	-38
07-17-05	X1.2	-75

In Fig. 9, we show a comparison between the integrated flux of X-class flares and the peak of the local geomagnetic-field disturbance. A weak correlation between the two data appears whenever the integrated flux is greater than 0.5; and, finally, in Fig. 10 we have a plot of geomagnetic field disturbance versus X-class flares.

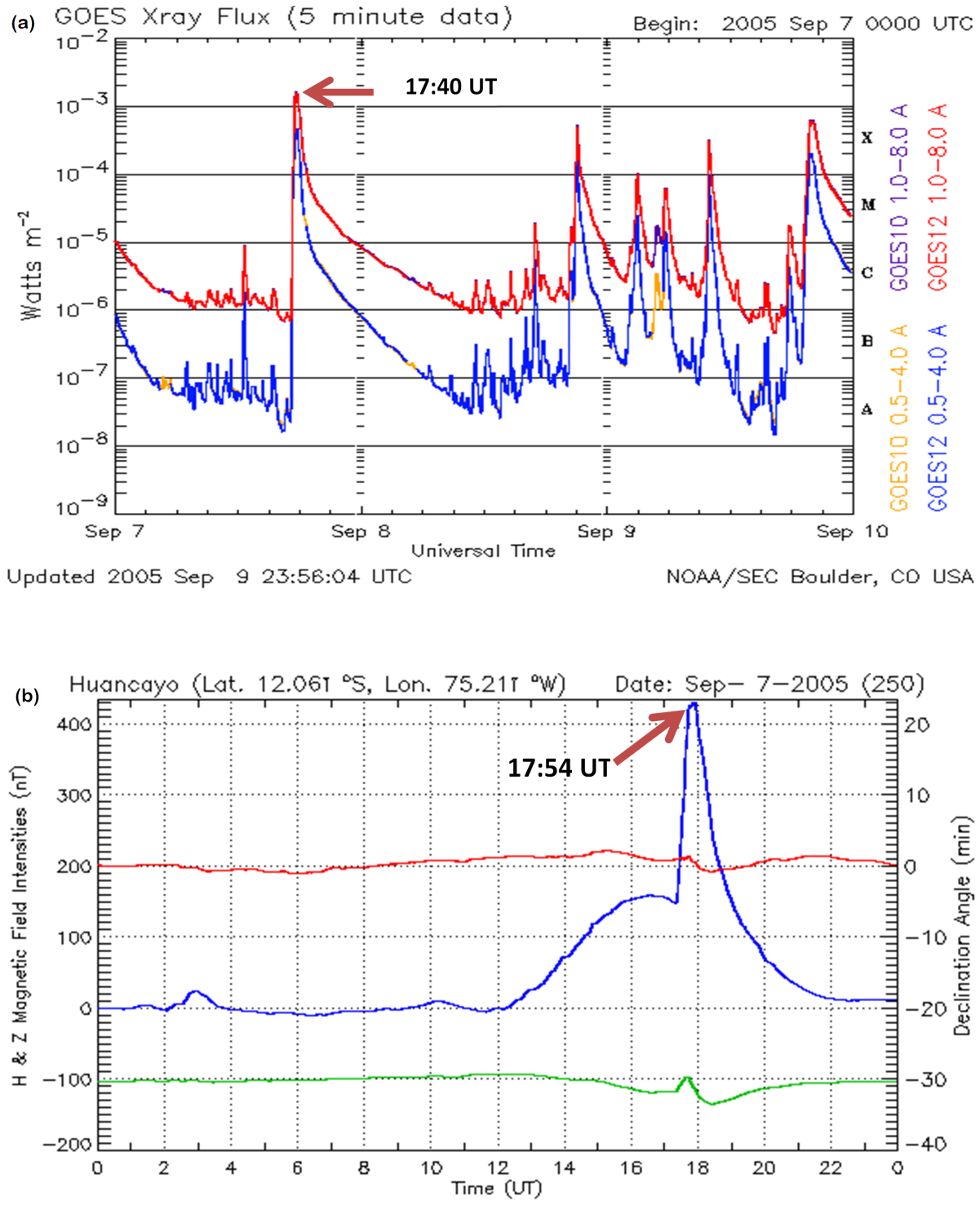

Fig. 6. **(a)** *An X17-class flare happened on September 7, 2005; the maximum peak recorded at 17:40 UT. The 1-8 Angstrom passband for GOES 10 X-ray flux is almost imperceptible (purple lines). Taken from NOAA/NWS Space Weather Prediction Center.* **(b)** *HGO magnetogram for the previously indicated date; the maximum peak recorded at 17:54 UT. The colors in this magnetogram have already been explained in Fig. 1.*

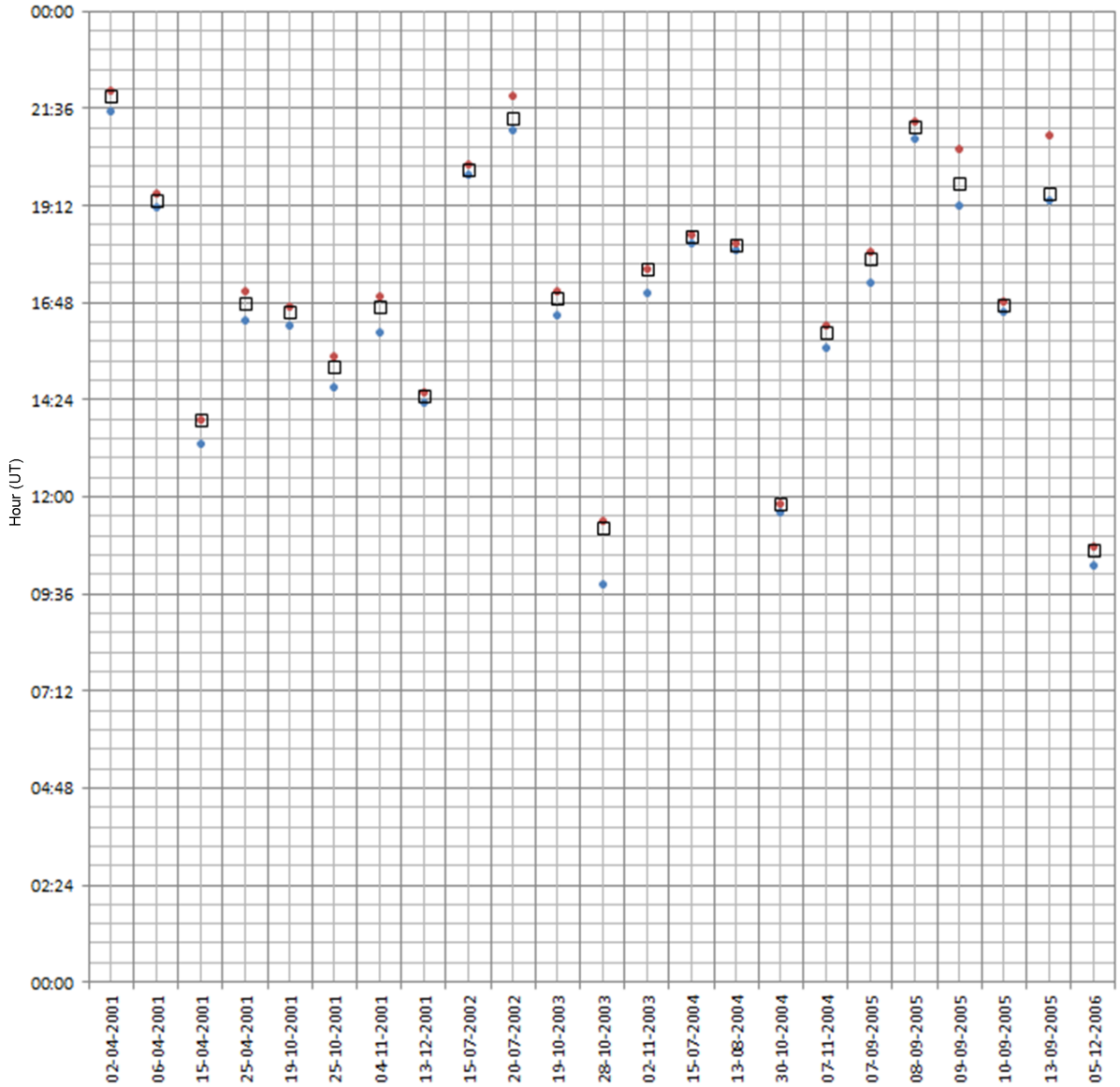

Fig. 7. *Start hour and end hour of X-class flares compared with the hour when the sudden disturbance of H appears in the HGO magnetograms. Blue circles stand for the start hour and red circles represent the end hour; white rectangles are the peak hours of H.*

4. CONCLUSIONS

For the period 2001-2010, we conclude that there is no relationship between the daily flare indices and the daily global-magnetic-activity indices. However, a peak overlapping appears when we consider the corresponding monthly indices which indicates that the solar flare events and the disturbance of the local geomagnetic field are not simultaneous.

For more than 80% of the X-class flares, a strong disturbance of the geomagnetic field is observed after two to three days. However, when we plotted the intensity of the disturbance versus the classification in X class, there was no relationship between them.

Some solar flares coincide with the disturbance peak of the geomagnetic field. In these cases, there is a weak correlation between the magnitude of the disturbance and the total flux of the solar flare for values higher than 0.5 of the total flux.

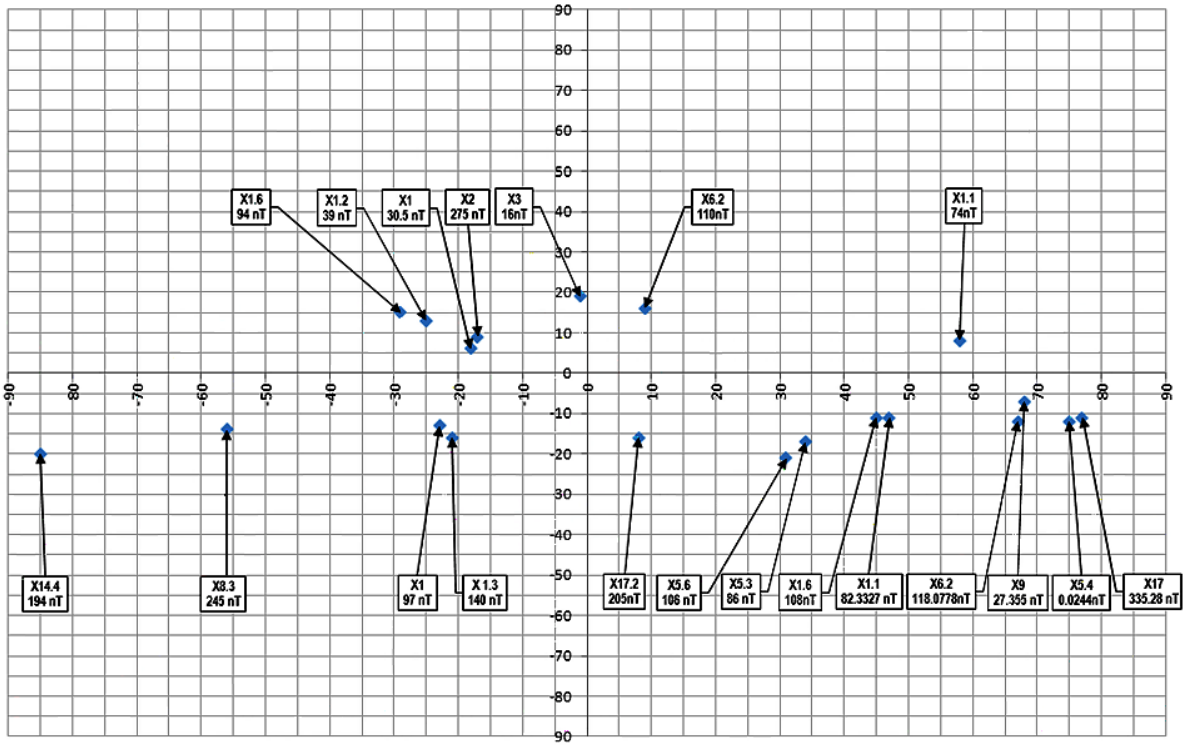

Fig. 8. *Location on the solar disk of flares appearing in Fig. 7.*

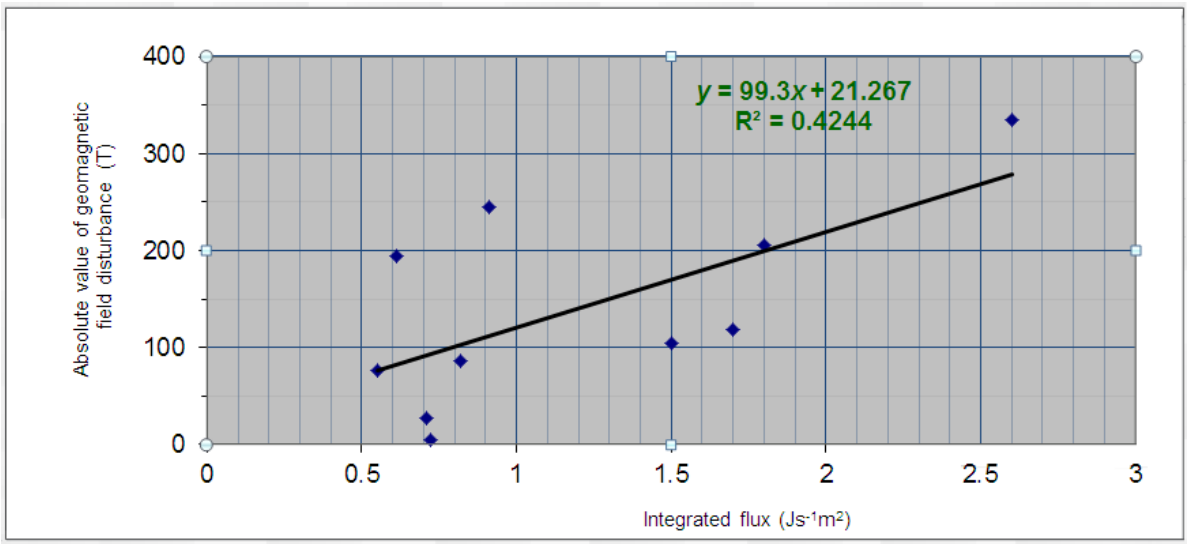

Fig. 9. *Geomagnetic field disturbance versus the integrated flux of X-class flares. Integrated flux means the X-rays emission in the region of the peak that we consider to be related to the local geomagnetic field.*

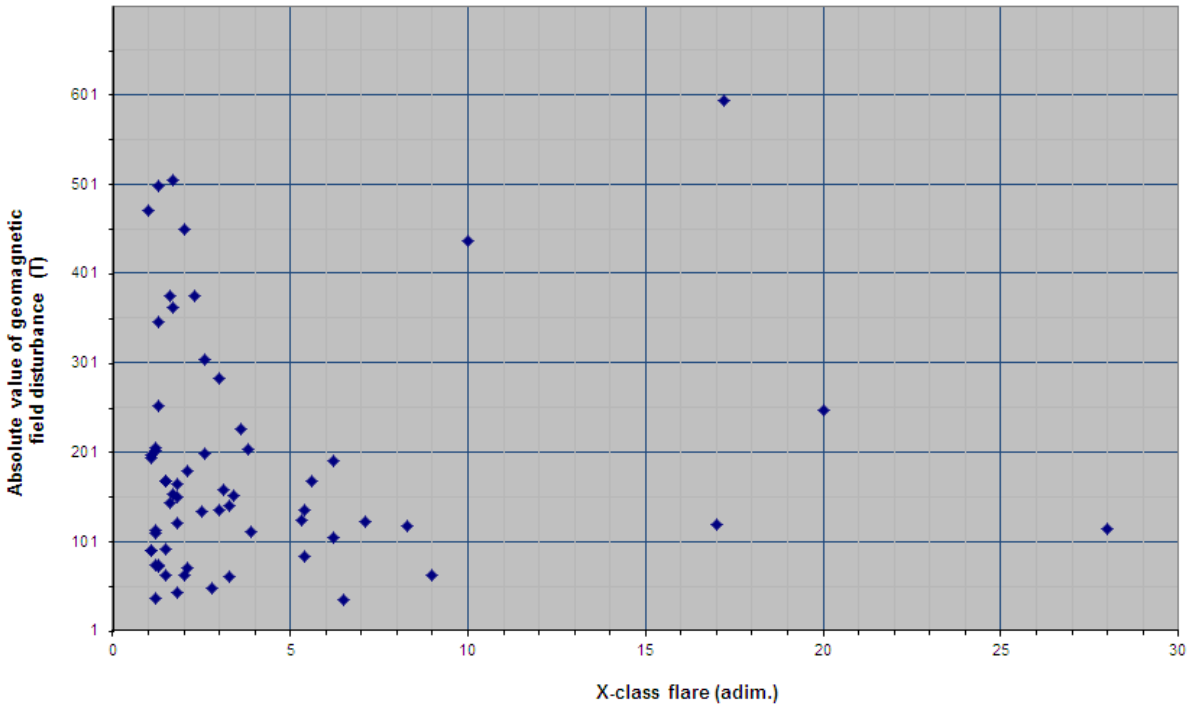

Fig. 10. *Geomagnetic field disturbance versus X-class flares.*

Acknowledgements – We earnestly thank J. Meléndez for his comments and suggestions, which helped to improve this investigation.

REFERENCES

Ataç, T. and Özgüç, A.: 1998, *Solar Phys.*, **180**, 397.
Bai, T. and Sturrock, P. A.: 1989, *Annu. Rev. Astron. Astrophys.*, **27**, 421.
Cliver, E. W. and Hudson, H. S.: 2002, *J. Atmos. Sol.-Terr. Phys.*, **64**(2), 231.
Cui, Y., Li, R., Zhang, L., He, Y. and Wang, H.: 2006, *Solar Phys.*, **237**(1), 45.
DACGSM: 2015, http://wdc.kugi.kyoto-u.ac.jp/qddays/index.html
Du, Z. and Wang, H.: 2012, *Res. Astron. Astrophys.*, **12**(4), 400.
Foukal, P. V.: 2004, Solar Astrophysics, 2nd edition, Wiley-VCH, Weinheim.
Giesecke, A. and Casaverde, M.: 1998, *Revista Geofísica*, **49**, 4.
Gosling, J. T.: 1993, *J. Geophys. Res.*, **98**(A11), 18937.
Howard, T. A. and Tappin, S. J.: 2005, *Astron. Astrophys.*, **440**, 373.
Kleczek, J.: 1952, *Publ. Inst. Centr. Astron.*, **22**, 1.
Knŏska, S. and Petrásek, J.: 1984, *Contr. Astron. Obs. Skalnaté Pleso*, **12**, 165.
Legrand, J. P. and Simon, P. A.: 1989a, *Ann. Geophys.*, **7**(6), 565.
Legrand, J. P. and Simon, P. A.: 1989b, *Ann. Geophys.*, **7**(6), 579.
Mayaud, P. N.: 1980, Geophysical Monograph 22, American Geophysical Union, Washington DC.
Meza, A., Van Zele, M. A. and Rovira, M.: 2009, *J. Atmos. Sol.-Terr. Phys.*, **71**(12), 1322.
NCEI: 2015, http://www.ncei.noaa.gov/find-data-by-category#Geomagnetism
NOAA-flares: 2015, http://www.ngdc.noaa.gov/stp/space-weather/solar-data/solar-features/solar-flares/index/flare-index/
NOAA-NGDC: 2015, http://www.ngdc.noaa.gov/stp/space-weather/solar-data/solar-features/solar-flares/x-rays/goes/
Rangarajan, G. K.: 1989, *Geomagnetism*, **3**, 323.
Remanan, R. and Unnikrishnan, K.: 2014, *Jour. Atm. Solar-Terr. Phys.*, **107**, 113.
Rosales Corilloclla, D., Vidal Safor, E. and Orihuela Lazo, S.: 2011, Yearbook - Huancayo Geomagnetic Data 2009, Instituto Geofísico del Perú and Radio Observatorio de Jicamarca, Lima.
Shea, M. A., Smart, D. F., McCracken, K. G., Dreschhoff, G. A. M. and Spence, H. E.: 2006, *Adv. Space Res.*, **38**(2), 232.
Siebert, M. and Meyer, J.: 1996, in "The Upper Atmosphere: Data Analysis and Interpretation", eds. W. Dieminger, G. K. Hartmann and R. Leitinger, Springer-Verlag, Berlin-Heidelberg, 887.
Stamper, R., Lockwood, M., Wild, M. N. and Clark, T. D. G.: 1999, *J. Geophys. Res. (Space Physics)*, **104**(A12), 28325.
Tsurutani, B. T., Slavin, J. A., Kamide, Y., Zwickl, R. D., King, J. H. and Russell, C. T.: 1985, *J. Geophys. Res. (Space Physics)*, **90**, 1191.
Youssef, M.: 2012, *NRIAG J. Astron. Geophys*, **1**(2), 172.

СУНЧЕВЕ ЕРУПЦИЈЕ И ВАРИЈАЦИЈА У ЛОКАЛНОМ ГЕОМАГНЕТНОМ ПОЉу: МЕРЕЊА СА УАНКАЈО ОПСЕРВАТОРИЈЕ У ПЕРИОДУ ОД 2001. ДО 2010. ГОДИНЕ

Rafael E. Carlos Reyes[1,2], Gabriel A. Gárate Ayesta[1] and Felipe A. Reyes Navarro[2]

[1] *Universidad Nacional del Callao, UNAC, Callao, Peru*

[2] *Universidad Nacional Mayor de San Marcos, UNMSM, Lima, Peru*

E–mail: *felipe.reyes@unmsm.edu.pe*

УДК 523.31-337 : 523.985.3

Стручни чланак

Проучавали смо локалну варијацију геомагнетног поља измерену на Уанкајо геомагнетној опсерваторији у Перуу, у периоду од 2001. до 2010. године. Првобитно смо тражили однос између SFI вредности која се свакодневно прикупља у Националном геофизичком центру за податке, NOAA, и одговарајућег геомагнетног индекса, али веза није установљена. Поређење између месечног индекса геомагнетне активности и просечне месечне вредности SFI индекса је даље омогућило посматрање временске корелације између ових просечних индекса. Из ове корелације следи да се Сунчеве ерупције не одражавају истовремено на одговарајуће магнетне индексе. Да бисмо истражили ову појаву, изабрали смо најинтензивније ерупције класе X, а затим посматрали поремећаје магнетног поља из магнетограма са Уанкајо геомагнетне опсерваторије. Пронашли смо неке поремећаје у локалном геомагнетном пољу у другом и трећем дану након одговарајуће Сунчеве ерупције, међутим није нађена корелација између величине поремећаја локалног геомагнетног поља и класе X Сунчевих ерупција. Коначно, примећени су неки поремећаји у локалном геомагнетном пољу који су истовремени са класом X Сунчевих ерупција, и они показују корелацију са укупним флуксом Сунчеве ерупције.